Altered Differentiation of Hepatocytes in a Transgenic Mouse Model of Hepatocarcinogenesis*

AKIKO ENOMOTO,[1,2] ERIC P. SANDGREN,[3] AND ROBERT R. MARONPOT[1]

[1]*Laboratory of Experimental Pathology, National Institute of Environmental Health Sciences, Research Triangle Park, North Carolina 27709,*
[2]*Laboratory of Pathology, Institute of Environmental Toxicology, Ibaraki 303-0043, Japan, and*
[3]*School of Veterinary Medicine, University of Wisconsin, Madison, Wisconsin 53706*

ABSTRACT

Transgenic mice carrying the SV40 T antigen (TAg) gene, which develop hepatocellular and biliary cell tumors by 4 mo of age, show ductular structures in the neonatal liver. Coexpression of c-*myc* with TAg increases the extent and persistence of ductular lesions and also accelerates tumor development. To analyze possible links between altered gene expression and cell differentiation and to determine the relationship between the ductular structures and tumor development in these mice, ductular cells in single (TAg) and bitransgenic (TAg × c-*myc*) mice were characterized for biliary and hepatocellular differentiation, transgene expression, and proliferation activity. The results show that the ductular cells in these transgenic mice have characteristics of biliary cells, including basement membrane formation, positive laminin staining, and bile duct-specific lectin (*Dolichos biflorus* agglutinin and peanut agglutinin) binding, and characteristics of hepatocytes, including albumin expression and ultrastructural features such as round nuclei with 1 or 2 nucleoli and well-developed cytoplasmic organelles. However, differences in transgene expression and cell proliferation between the ductular cells and nonductular hepatocytes were not apparent. Thus, the ductular cells could not be defined as tumor progenitor cells in these mouse livers. However, this model suggests that manipulation of gene expression can alter differentiation of hepatic parenchymal cells.

Keywords. Liver; neoplasms; ductular hepatocytes; cell differentiation; cell proliferation; bitransgenic mice

INTRODUCTION

Hepatocytes have been shown to form ductlike structures in some diseases. In humans, ductular hepatocytes have been reported in cases of alcoholic and cholestatic liver diseases, fulminant hepatitis, liver allograft rejection, and massive hepatic necrosis (17, 27, 30–32). In rats, ductular cells have been identified following treatment with chemicals (e.g., furan, D-galactosamine, carbon tetrachloride, and N-2-acetylaminofluorene in a choline-deficient diet) with or without bile duct ligation (5, 7, 14, 25, 26). In most instances, either extensive or chronic loss of hepatic parenchyma appears to be a necessary requisite for the appearance of ductular structures. In many of these cases, the ductular cells show characteristics of both hepatocytes and biliary cells and have sometimes been referred to as intermediate cells (5, 14, 17, 27, 30).

Transgenic mice carrying the simian virus 40 (SV40) T antigen (TAg) gene fused to an albumin promoter/enhancer develop hepatocellular and biliary cell tumors at 3 or 4 mo of age (22). Examination of livers from these mice revealed the presence of ductular structures in neonates at 1 and 2 wk of age (8). Coexpression of a second transgene, c-*myc*, with TAg accelerated tumor development dramatically (22) and also resulted in an increase in the extent and persistence of the ductular structure formation (8). In these bitransgenic mice, some hepatocellular and biliary cell tumors coexisted with the ductular cells. Such phenotypic changes in hepatocytes prior to and/or during initial phases of tumor development led to speculation that the duct formation might be a step in the carcinogenic process underlying some tumors in this hepatocarcinogenesis model.

Histomorphologic features of a cell reflect differential gene expression. The effects of altered gene expression, however, are not necessarily limited to the change in morphology but may also involve other fundamental properties of the cell, such as growth and differentiation. The purposes of this study were to (a) analyze the possible links between altered gene expression and cell differentiation and (b) determine the relationship between the appearance of ductular hepatocytes and the development of neoplasia in this hepatocarcinogenesis model.

MATERIALS AND METHODS

Transgenic Mice. Animals carrying a single transgene, i.e., SV40 TAg or c-*myc* gene fused to an albumin promoter/enhancer (AL), or bitransgenes, i.e., AL-TAg × AL-*myc*, were used for the study. Details of the phenotype of each line of mouse have been described (8, 22). Transgene-negative littermates were used as controls.

Histopathology. Animals carrying single transgenes or bitransgenes were euthanized at 1, 2, 3, or 4 wk of age by cervical dislocation or CO_2 asphyxiation (4–24 mice/line/age, see Table I), and livers were removed and fixed in 10% neutral buffered formalin or 4% paraformaldehyde. A part of each tissue was embedded in paraffin, sectioned, stained with hematoxylin and eosin (H&E) according to standard methods, and examined microscopically.

* Address correspondence to: Dr. Akiko Enomoto, Laboratory of Pathology, Institute of Environmental Toxicology, 4321 Uchimoriya-machi, Mitsukaido-shi, Ibaraki 303-0043, Japan; e-mail: enomoto@mxg.meshnet.or.jp.

0192-6233/98$3.00+$0.00

TABLE I.—Incidence[a] of ductular structures in transgenic mouse livers.

Mouse age (wk)	Transgenes			
	AL-TAg	AL-TAg × AL-*myc*	AL-*myc*	None
1	2/5[a] (40)	7/9 (78)	0/7	0/8
2	9/24 (38)	17/18 (94)	0/11	0/17
3	0/7	8/9 (89)	0/10	0/5
4	0/12	0/7	0/4	0/5

[a] Number of animals with ductular structures/number of animals examined (%).

Electron Microscopy. Liver tissues were sampled from animals carrying AL-TAg or AL-TAg × AL-*myc* at 7, 14, or 24 days of age (2 or 3 mice/line/age). A part of each liver was trimmed into small pieces and fixed in a glutaraldehyde/paraformaldehyde-mixed solution (2.6% glutaraldehyde, 2.0% paraformaldehyde, and 3.0% sucrose in 0.1 M phosphate buffer, pH 7.4) at 4°C. The tissues were processed according to routine methods, stained with uranyl acetate and lead citrate, and examined in a Zeiss EM 10C/CR electron microscope.

Lectin Histochemistry. Binding sites for 2 kinds of lectins, *Dolichos biflorus* agglutinin (DBA) and peanut agglutinin (PNA), were detected histochemically on formalin-fixed tissues from AL-TAg and AL-TAg × AL-*myc* mice at 1, 2, or 3 wk of age (2 mice/line/age). Deparaffinized sections were incubated in 3% hydrogen peroxide for 15 min and in phosphate-buffered saline containing 1% milk and 1% bovine serum albumin for 20 min, and then biotin-labeled lectins (Sigma Chemical Co., St. Louis, MO) were applied at a concentration of 30 μg/ml for 30 min followed by streptavidin–biotin complex (Biogenex Laboratories, San Ramon, CA) for 30 min. Signal was detected using diaminobenzidine (Sigma Chemical Co.) as the chromogen. The specificity of lectin binding was confirmed by preincubation of tissues with N-acetyl-D-galactosamine (Sigma Chemical Co.) or D(+)-galactose (Sigma Chemical Co.) before incubation with DBA or PNA, respectively.

Immunohistochemistry. Immunohistochemical staining for TAg was performed on formalin-fixed tissues from AL-TAg and AL-TAg × AL-*myc* mice at 1, 2, 3, or 4 wk of age (3 mice/line/age) as described previously (8). For detection of myc protein, sections of formalin-fixed, paraffin-embedded tissues from single transgenic and bitransgenic mice at 1, 2, 3, or 4 wk of age (3 mice/line/age) were digested with 0.1% trypsin (Sigma Chemical Co.) in distilled water containing 0.1% calcium chloride for 20 min at 37°C and incubated in 3% hydrogen peroxide for 15 min. A rabbit polyclonal antibody to synthetic Myc peptide (OA-11–802, Cambridge Research Biochemicals, London, UK) was applied on the tissues at a dilution of 1:400 (2.5 μg/ml IgG) for 60 min at room temperature. The remainder of the staining was performed using Vectastain Elite ABC Kit (rabbit IgG, Vector Laboratories, Burlingame, CA). Sections of normal mouse colon were used as positive controls (16, 29). As a negative control, the primary antibody was replaced by normal rabbit IgG. Immunohistochemical staining for laminin was performed for the same animals as those used for lectin histochemistry. Formalin-fixed, paraffin-embedded tissues were stained basically as described above except that protease (type XXIV, 4 mg/ml, Sigma Chemical Co.) and Vectastain ABC Kit (rabbit IgG) were used instead of trypsin and Vectastain Elite ABC Kit, respectively; the digestion by protease was performed for 15 min at room temperature. Primary antibody, a rabbit polyclonal anti-laminin antibody (Sigma Chemical Co.), was applied on the tissues at a dilution of 1:200 overnight at 4°C.

In situ Hybridization. A DNA probe of 668 bp, which overlaps the *Hin*dIII region of mouse albumin DNA used for *in situ* hybridization previously (2, 4, 12, 21), was generated using 2 rounds of polymerase chain reaction (PCR). Primers used were 5′-GTA TGC AGA AGT TTG GAG AGA-3′ (upper) and 5′-CAC GAG AGT TGG GGT TGA CAC-3′ (lower). Fifty microliters of reaction solution for the first round of PCR contained 0.4 μM of each primer, 8.2 μg of mouse liver cDNA library as a template, 0.2 mM of dNTPs, and 2 units of Ampli*Taq* polymerase (Perkin-Elmer, Foster City, CA) in 1× PCR buffer containing 1.5 mM $MgCl_2$. After incubation for 5 min at 94°C, *Taq* polymerase was added, and 35 cycles of PCR were performed under the following conditions: 1 min at 94°C, 1.5 min at 55 °C, and 1.5 min at 72°C, followed by 7 min at 72°C at the end of the last cycle for extension. The product was purified using a QIAquick Gel Extraction Kit (QUIAGEN, Chatsworth, CA), and the sequence was confirmed using an automated DNA sequencer (model 373A, Applied Biosystems, Foster City, CA). A second round of PCR was performed under the same conditions as the first round except that 150 ng of the purified product of the first round of PCR was used as a template, 0.07 mM of dUTP was replaced by digoxigenin (DIG)-11-dUTP (Boehringer-Mannheim, Indianapolis, IN), the cycle number was 10–30, and the final extension step was omitted. The DIG-labeled PCR product was used as a probe for *in situ* hybridization without further purification. As a negative control, the same size (668 bp) of probe for the murine heat-shock protein 70.2 gene (gift from Dr. Gotoh), which is expressed exclusively in the adult mouse testis (19), was used.

For *in situ* hybridization, sections of formalin-fixed, paraffin-embedded tissues from AL-TAg and AL-TAg × AL-*myc* mice at 1, 2, or 3 wk of age (2 mice/line/age) were digested with proteinase K at concentrations of 10–100 μg/ml; the temperature and the time for digestion were changed depending on the age of animals because tissues became more resistant to digestion with age. After digestion, the sections were refixed with 4% paraformaldehyde for 5 min and incubated with a prehybridization solution containing 50% deionized formamide and 0.3 M NaCl for ≥10 min, and then 20 μl of hybridization solution containing 5 ng/μl of probe DNA, 0.3 M NaCl, 50% deionized formamide, 1× Denhardt's solution, 20 mM Tris (pH 8.0), 5 mM EDTA, 10% dextran sulfate, 500 ng/μl tRNA, and 500 ng/μl salmon sperm DNA was applied. The slides with glass coverslips were incubated in a humidified chamber for 10–15 min at 100 °C to denature both probe DNA and tissue mRNAs and then kept overnight at 50°C. After hybridization, the tissues were rinsed in 2× standard saline citrate (SSC) for 3 min at

TABLE II.—Labeling index (LI) for livers of single transgenic and bitransgenic mice treated with BrdU at 14 days of age. Statistical analyses were not performed because of small group sizes.

Time after BrdU administration	Transgenes			
	AL-TAg	AL-TAg × AL-*myc*	AL-*myc*	None
2 hr				
n	3	6	5	2
LI (%)[a]				
Centrilobular	17.8 ± 1.1	25.6 ± 2.2	4.9 ± 1.7	4.4
Periportal	11.8 ± 2.2	15.5 ± 3.2	3.7 ± 1.3	3.6
Whole lobule	14.9 ± 1.7	20.8 ± 1.4	4.3 ± 1.4	3.9
3 days				
n	5	5	9	5
LI	ND[b]	ND	ND	ND
7 days				
n	12	2	8	6
LI	ND	ND	ND	ND

[a] For n ≧ 3, mean ± SD; for n = 2, mean only.
[b] ND = not determined.

room temperature and washed twice in 0.1× SSC for 1 hr at 60°C. Signal was detected using alkaline phosphatase-conjugated anti-DIG (Boehringer Mannheim) with nitroblue tetrazolium/5-bromo-4-chloro-3-indolyl phosphate as the chromogen. Tissues were counterstained with 0.02% fast green FCF and Gill's hematoxylin and mounted with aqueous mounting medium.

Cell Proliferation Analysis. Bromodeoxyuridine (BrdU, 30 mg/kg, ip) was administered to 2-wk-old mice carrying single transgenes or bitransgenes, and the animals were euthanized 2 hr, 3 days, or 7 days after BrdU administration (2–12 mice/line/age, see Table II). Liver tissues were removed and fixed in 4% paraformaldehyde, and BrdU incorporation was detected immunohistochemically as described previously (28) using rat monoclonal BrdU antibody, MAS250 (Accurate Chemical and Scientific Corp., Weatbury, NY). For each liver from animals euthanized 2 hr after BrdU administration, a BrdU labeling index (LI = number of BrdU positive nuclei/total number of nuclei × 100) was obtained by counting ≥1,000 hepatocytes in the microscopic fields consisting of a minimum 5 centrilobular and 5 periportal areas selected at random. For those euthanized 3 or 7 days after BrdU administration, distribution pattern of positive BrdU staining was examined microscopically, but LIs were not obtained.

RESULTS

Histopathology

Ductlike structures were found in mice carrying AL-TAg alone and in those carrying AL-TAg × AL-*myc* (Table I). The incidence, distinctiveness of the morphological features, and temporal persistence of these ductular structures were different between the single transgenic and bitransgenic mice.

In mice carrying AL-TAg alone, multiple small spaces, consistent with bile canaliculi and delimited by contiguous hepatocytes, were present at the periphery of liver lobes at 1 wk of age (Fig. 1). At 2 wk of age, the hepatocytes surrounding these spaces had a more discrete ductular pattern (Fig. 2). Ductular structures were seen also in centrilobular areas. At 3 wk of age, however, livers were occupied by contiguous hepatocytes with varying degrees of dysplasia but without discrete hepatic cords, and ductular hepatocytes were no longer present. Focal proliferative lesions of biliary cells and hepatocytes were first seen at 4 and 6 wk, respectively, within the background of dysplastic hepatocytes; biliary and hepatocellular tumors were first observed at 6 and 8 wk, respectively (8).

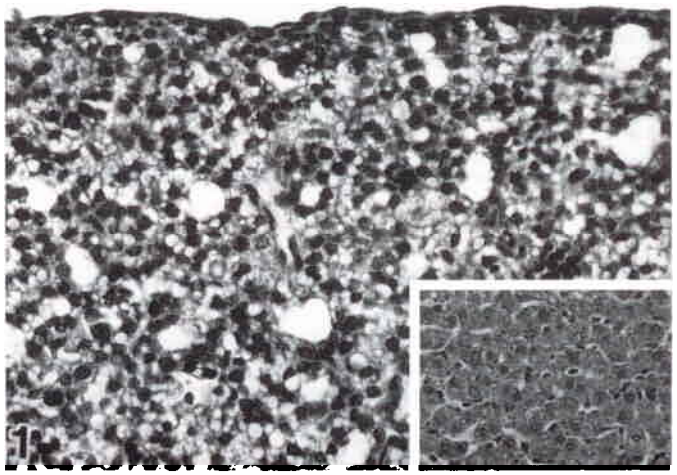

FIG. 1.—Multiple small spaces at the periphery of the liver lobe from a 1-wk-old AL-TAg mouse. H&E. ×340. *Inset.* Normal liver from a transgene-negative littermate of the same age. H&E. ×170.

In contrast to the mice carrying AL-TAg alone, mice coexpressing AL-*myc* with AL-TAg had more distinct ductular structures lined by hepatocytes, and these occupied a larger proportion of the liver and in centrilobular areas (Fig. 3); in some cases, entire liver lobules were occupied by the ductular structures. The cells lining the ductules were more basophilic than were nonductular he-

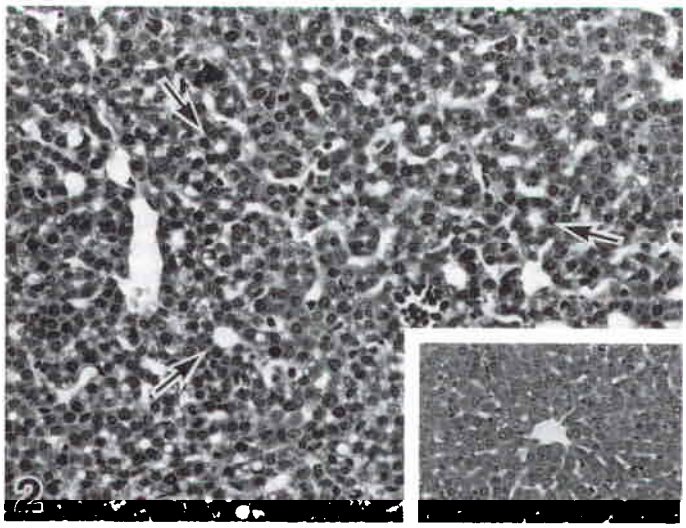

FIG. 2.—Ductular arrangement of some hepatocytes (arrows) in the liver from a 2-wk-old AL-TAg mouse. H&E. ×270. *Inset.* Normal liver from a transgene-negative littermate of the same age. H&E. ×140.

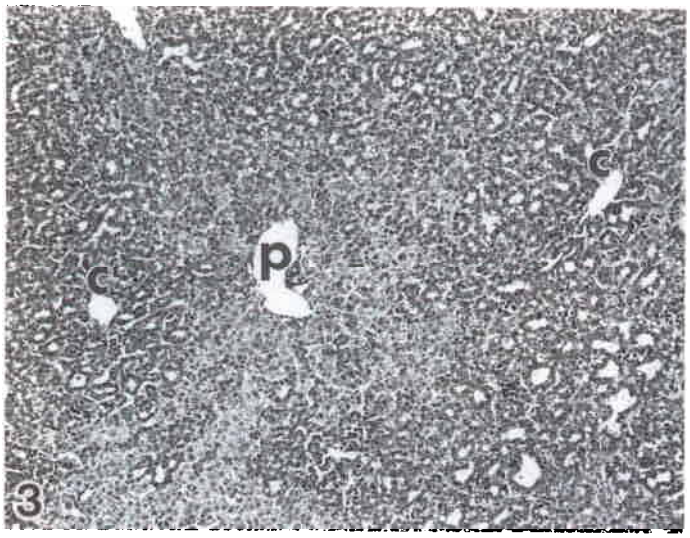

FIG. 3.—Centrilobular distribution of ductular hepatocytes in the liver from a 2-wk-old AL-TAg × AL-*myc* mouse. C = central vein; P = portal vein. H&E. ×90.

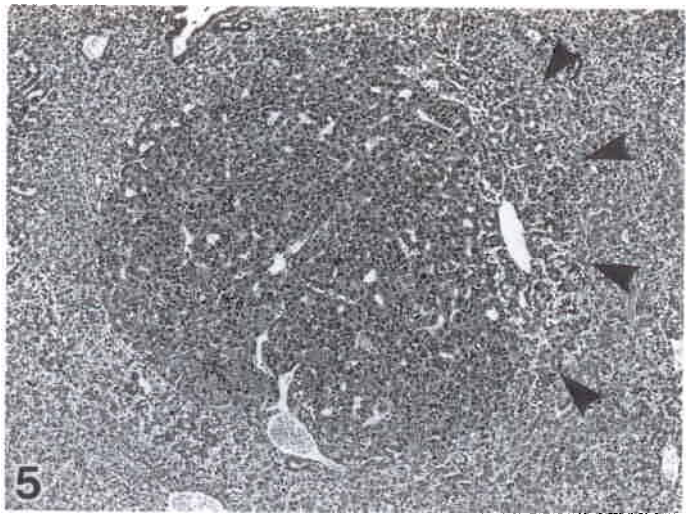

FIG. 5.—Focal proliferation of hepatocytes contiguous to a ductular area (arrowheads) in the liver from a 3-wk-old AL-TAg × AL-*myc* mouse. H&E. ×85.

patocytes but still had morphological features of hepatocytes in H&E-stained sections (Fig. 4). Unlike the ductular structures in single transgenic AL-TAg mice, the ductular lesions were still present in 8 of 9 bitransgenic mice examined at 3 wk of age. Furthermore, proliferative focal lesions of biliary cells were first seen at 1 wk of age and those of hepatocytes at 2 wk in the bitransgenic mice; cholangiolar and hepatocellular tumors developed at 3 wk of age (8). Some of these lesions were located in or were contiguous with the ductular areas (Figs. 5 and 6). Biliary cells in the proliferative lesions were columnar, had hyperchromatic, elongated nuclei with a high nucleus/cytoplasm ratio, and were distinct from the cells forming the ductular structures.

Severe hepatic damage was not seen in either line of mouse although apoptotic cells/bodies, which became apparent at 2 wk of age, increased in number with age in both lines. There were no ductular lesions in livers from mice carrying AL-*myc* alone or in those from transgene-negative littermates at any age examined (Table I).

Ultrastructural Characteristics

Cells forming ductular structures had ultrastructural characteristics of both hepatocytes and of biliary cells. In normal livers from transgene-negative littermates, bile canaliculi between contiguous hepatocytes had a small lumen filled with microvilli (Fig. 7). The lumen of ductular structures in transgenic mouse liver was distended, irregular in shape, contained scanty microvilli, and was surrounded by 3 to >10 cells (Figs. 8 and 9). In some instances, basement membrane was detected between duct-forming cells and adjacent nonductular hepatocytes

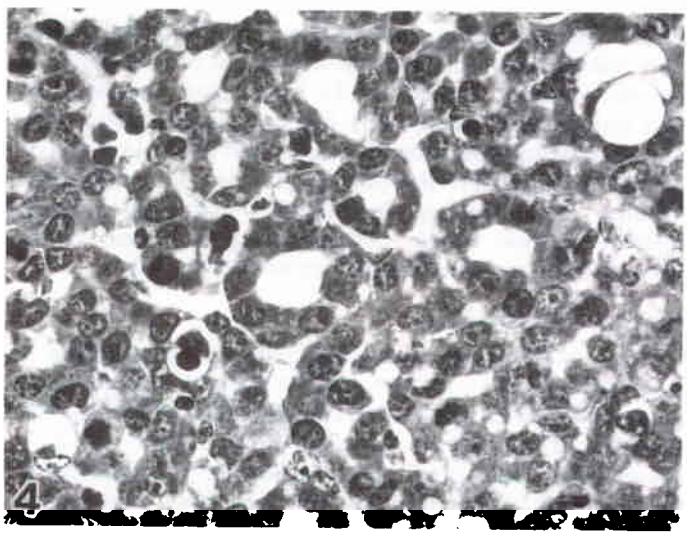

FIG. 4.—Higher magnification of ductular cells from the same liver as shown in Fig. 3. H&E. ×680.

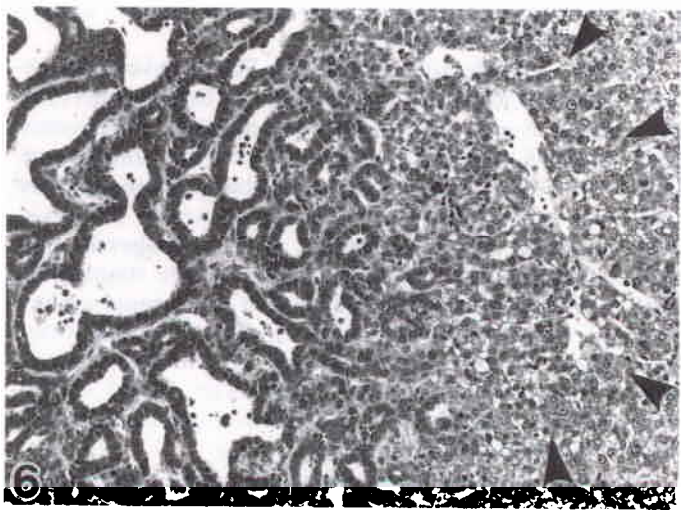

FIG. 6.—A biliary cell tumor contiguous to a ductular area (arrowheads) in the liver from a 3-wk-old AL-TAg × AL-*myc* mouse. H&E. ×170.

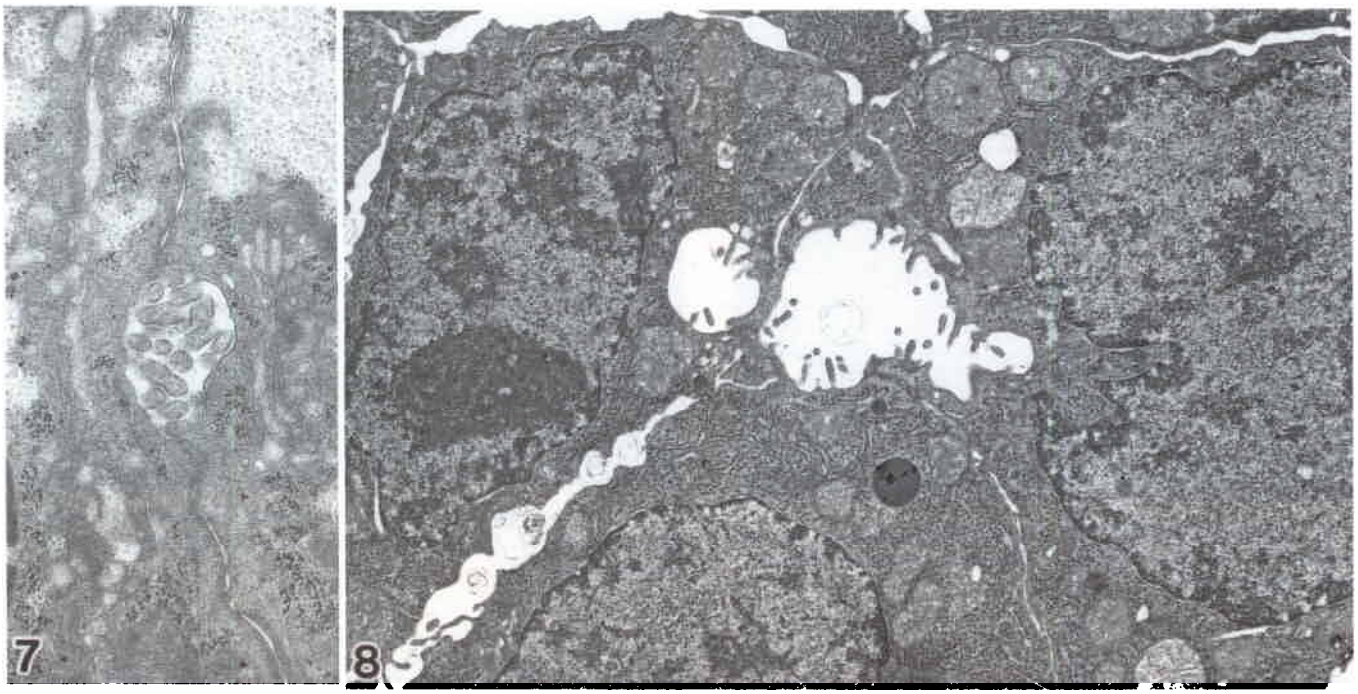

FIG. 7.—Electron micrograph of a normal bile canaliculus from a 2-wk-old nontransgenic littermate. The canaliculus has a small lumen of regular form filled with microvilli. Uranyl acetate and lead citrate. ×21,000.

FIG. 8.—Electron micrograph of an early ductular structure from a 1-wk-old AL-TAg × AL-*myc* mouse. Bile canaliculus is distended and contains scanty microvilli. Uranyl acetate and lead citrate. ×8,400.

(Fig. 10). The cells forming the ductules, however, also had hepatocytic features, including centrally placed round nuclei with 1 or 2 nucleoli, numerous round mitochondria, well-developed rough endoplasmic reticulum and free ribosomes, and occasional lysosomes (Figs. 8 and 9).

Histochemical Characterization

Morphological and/or functional markers of biliary cells (bile duct-specific lectin binding and laminin) and of hepatocytes (albumin) were detected as follows in cells forming ductular structures.

Lectins. Two lectins, DBA and PNA, have been reported to bind to biliary cells but not to hepatocytes (33). In normal livers from transgene-negative littermates, DBA or PNA binding was detected on the luminal surface of bile ducts and/or in the cytoplasm of biliary cells; there was no positive staining in hepatocytes. However, in livers from single transgenic and bitransgenic mice carrying AL-TAg, weak but clearly positive staining for DBA and PNA was detected either on the luminal surface or in the cytoplasm of some cells forming ductular structures (Figs. 11 and 12). No binding sites for these lectins were detected in nonductular hepatocytes. There was no recognizable difference in the staining pattern between single transgenic and bitransgenic mice.

Laminin. In livers from single transgenic and bitransgenic mice carrying AL-TAg, laminin was detected around each ductular structure (Fig. 13) and around normal bile ducts. Increased staining intensity was associated with the distinctiveness of ductular structures. There was no staining for laminin around hepatocytes that were not forming ducts. When ductular structures were not detected in the AL-TAg single transgenic mice at 3 wk of age, laminin was undetectable except for that surrounding normal bile ducts, whereas it remained positive around the more persistent ductular structures in the livers from bitransgenic mice. Positive staining for laminin was clearly seen around hyperplastic and neoplastic bile ducts in older AL-TAg and bitransgenic mice.

Albumin. In livers from nontransgenic littermates, albumin mRNA was detected in almost all hepatocytes, with highest staining intensity in periportal areas; albumin mRNA was not detected in normal biliary cells under the staining conditions. In livers from the AL-TAg and bitransgenic mice, cells forming ductular structures and nonductular hepatocytes were both albumin positive; even in cases where the ductular lesions occupied entire lobules, cells forming the ductules expressed albumin mRNA whereas biliary cells in the portal areas of the same sections were albumin negative (Fig. 14).

Transgene Expression

TAg. The staining intensity, pattern, and duration of TAg expression were the same between the single transgenic and bitransgenic mice carrying AL-TAg. TAg protein was present in the nuclei of most hepatocytes in 1-wk-old mice, including those hepatocytes surrounding the small spaces at the periphery of liver lobes (the earliest change of ductular structure formation). TAg-positive cells, however, gradually decreased with age. At 2 wk, TAg protein was detected mainly in centrilobular areas

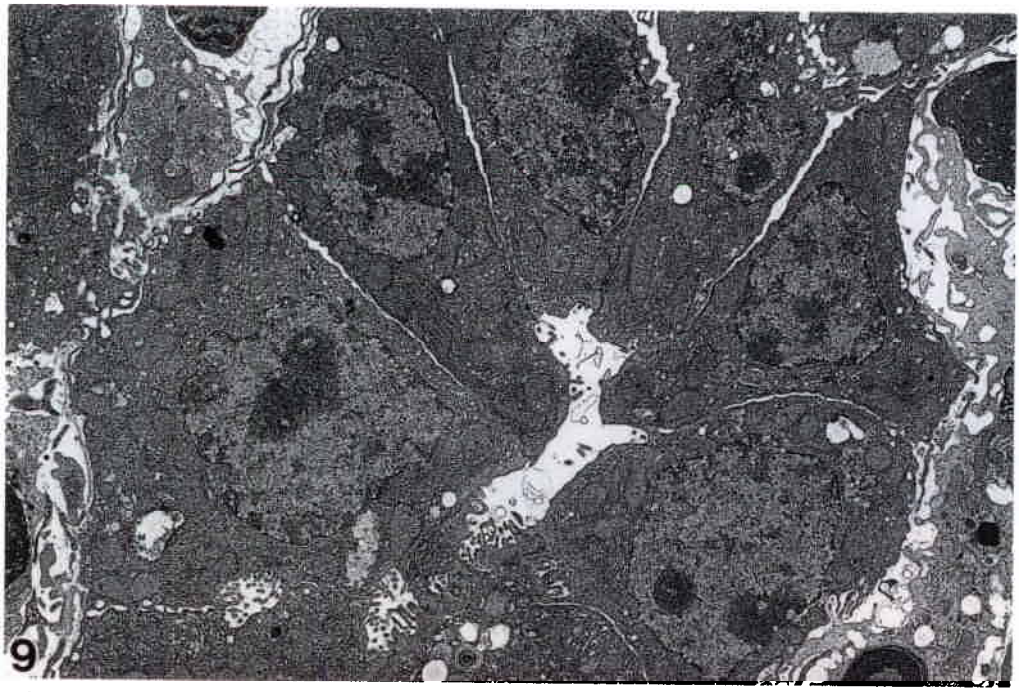

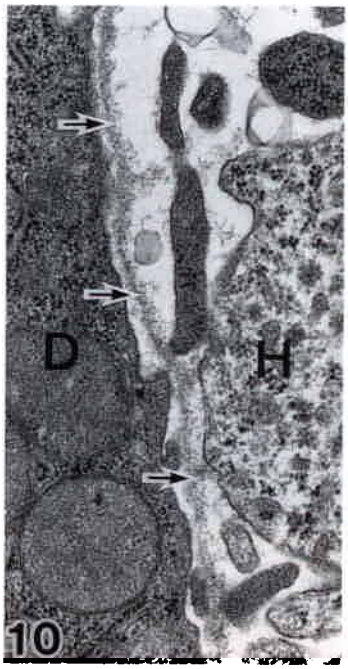

FIG. 9.—Electron micrograph of a ductular structure surrounded by several cells in the liver from a 1-wk-old AL-TAg × AL-*myc* mouse. Uranyl acetate and lead citrate. ×4,500.

FIG. 10.—Electron micrograph of a basement membrane (arrows) between a ductular cell (D) and nonductular hepatocyte (H). Uranyl acetate and lead citrate. ×27,500.

(Fig. 15) where, in some livers, ductular structures were present. There was, however, no clear difference in TAg expression between cells forming ductular structures and nonductular hepatocytes. By 3 wk, most hepatocytes were TAg negative except for a small number of cells around central veins. TAg-positive biliary cells were also seen in some cases.

Myc. Myc protein was detected in the nuclei of most hepatocytes at 1–4 wk of age in both nontransgenic and transgenic mouse livers (Fig. 16). No detectable difference in *myc* expression was present among the livers from animals carrying AL-*myc* or AL-TAg × AL-*myc* and transgene-negative littermates. Differences in *myc* expression between cells forming ductular structures and nonductular hepatocytes were not apparent.

Cell Proliferation Activity

The greatest degree of cell proliferation was seen in bitransgenic mice carrying AL-TAg × AL-*myc* followed by AL-TAg single transgenic mice, as shown by BrdU LIs from those mice euthanatized 2 hr after BrdU administration (Table II). The LI in the centrilobular areas in bitransgenic mice was 1.7 times higher than that in the periportal areas; the same pattern of BrdU positivity was seen in livers from AL-TAg single transgenic mice. There were no recognizable differences in BrdU positivity between cells forming ductular structures and nonductular hepatocytes in single transgenic and bitransgenic mouse livers, although a BrdU LI was not obtained separately for these 2 types of cells because of the difficulty of distinguishing ductular and nonductular cells clearly in sections stained for BrdU. Active proliferation of cells in bitransgenic mouse livers and, to a lesser extent, in the AL-TAg mouse livers was also indicated by apparent loss of BrdU-positive cells in their livers by 3 days after BrdU administration. In animals euthanatized 3 or 7 days after a pulse dose of BrdU, solid positive (brown) staining for BrdU was lost in many hepatocytes in single transgenic and bitransgenic mice carrying AL-TAg, and instead fine or coarse patches of brown staining were present in some hepatocellular nuclei, whereas persistent solid brown staining was detected in livers from AL-*myc* and transgene-negative littermates at the same time points.

DISCUSSION

We have demonstrated the transient occurrence of ductular structures in livers of mice carrying the AL-TAg transgene and shown that the ductular cells have morphological, histochemical, and functional characteristics of both hepatocytes and biliary cells. The ductular structures appeared to develop as dilated bile canaliculi between contiguous hepatocytes, and the cells forming these ductules exhibited evidence of biliary differentiation, including basement membrane, positive laminin staining, and bile duct-specific lectin binding, while maintaining features of hepatocytes, including albumin synthesis and ultrastructural characteristics such as round nuclei with 1 or 2 nucleoli and well-developed cytoplasmic organelles. Similar duct formation previously documented in humans (17, 27, 30–32) and animals (5, 7, 14, 25, 26) is typically associated with extensive or continuous loss of hepatic parenchyma. However, the livers of AL-TAg mice in the present study lacked evidence of massive hepatic cell loss, suggesting that this altered dif-

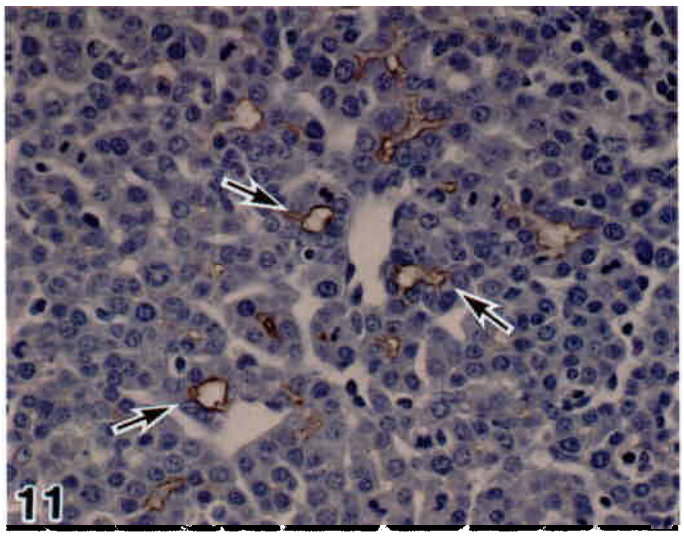

FIG. 11.—DBA binding on the luminal surface of ductular cells (arrows) in the liver from a 2-wk-old AL-TAg × AL-*myc* mouse. Lectin histochemistry. ×370.

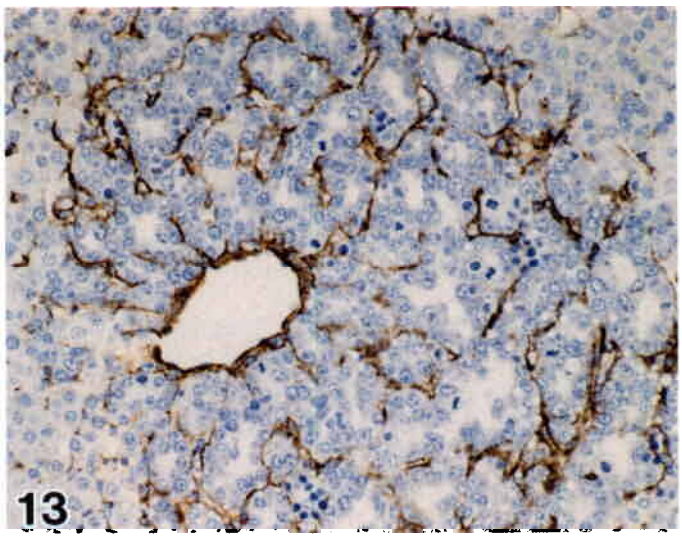

FIG. 13.—Laminin surrounding ductules in the liver from a 2-wk-old AL-TAg × AL-*myc* mouse. Immunohistochemical staining for laminin. ×220.

ferentiation is directly or indirectly attributed to the AL-TAg transgene and is not secondary to hepatic damage.

Whether TAg expression led to the altered differentiation by directly affecting cellular differentiation processes or by other indirect mechanisms is not known. The temporal and topographic occurrence of ductular structures appeared to be associated with TAg expression. Both ductular structures and TAg expression were detectable mainly at 1–2 wk of age; although TAg expression diminished with age, it remained longer in centrilobular areas than in periportal areas, the distribution pattern of which was consistent with that of ductular structures. However, ductular structures have not been reported in livers of other lines of mice carrying TAg (1, 3, 6, 11, 20, 23, 24) despite the fact that bile duct proliferation and/or biliary cell tumors have been reported in some of these mouse lines (1, 20, 23, 24). The early and transitory appearance of ductular structures might be one of the reasons for the absence of such reports. Another possibility is that the disrupted expression of some gene(s), caused by the insertion of the transgene (10, 18), but not the TAg gene itself, triggered the ductular formation in the present model. The present study could not reveal whether TAg itself was the causative factor for these phenotypic changes; however, this model appears to demonstrate that a genetic alteration introduced into the mouse genome could affect differentiation of hepatic cells.

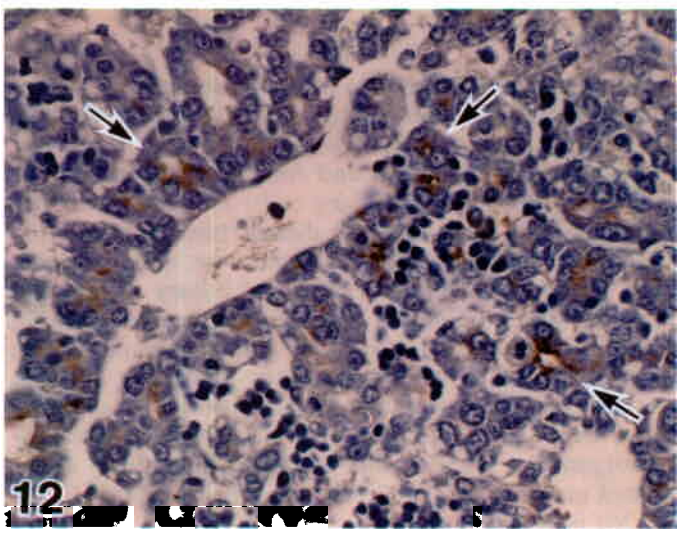

FIG. 12.—PNA binding on the luminal surface and in the cytoplasm of ductular cells (arrows) in the liver from a 2-wk-old AL-TAg × AL-*myc* mouse. Lectin histochemistry. ×370.

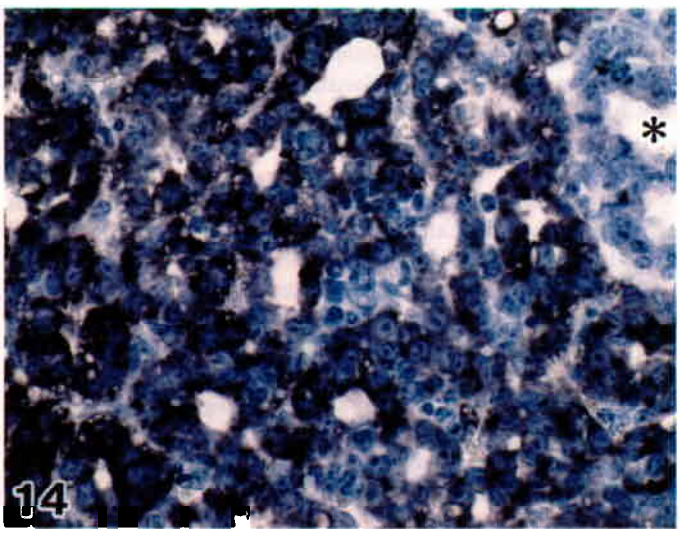

FIG. 14.—Albumin expression (black stain) in ductular cells in the liver from a 2-wk-old AL-TAg × AL-*myc* mouse. Bile duct (*) cells are albumin negative. *In situ* hybridization for albumin mRNA. ×440.

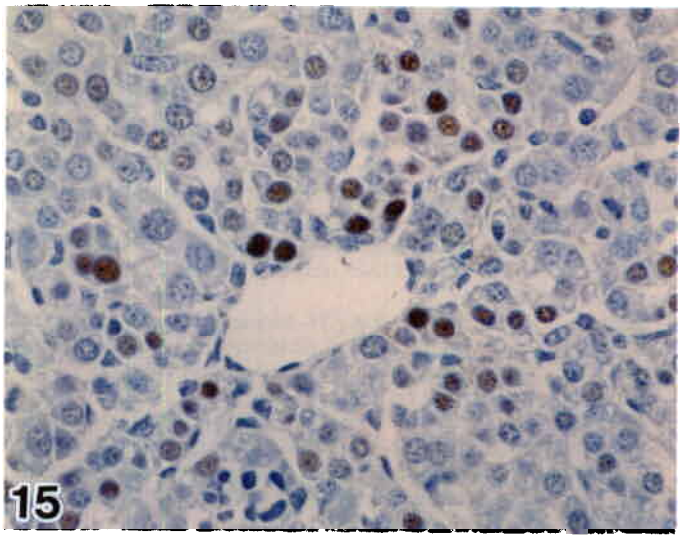

FIG. 15.—TAg expression in centrilobular hepatocytes in the liver from a 2-wk-old AL-TAg mouse. Immunohistochemical staining for TAg protein. ×440.

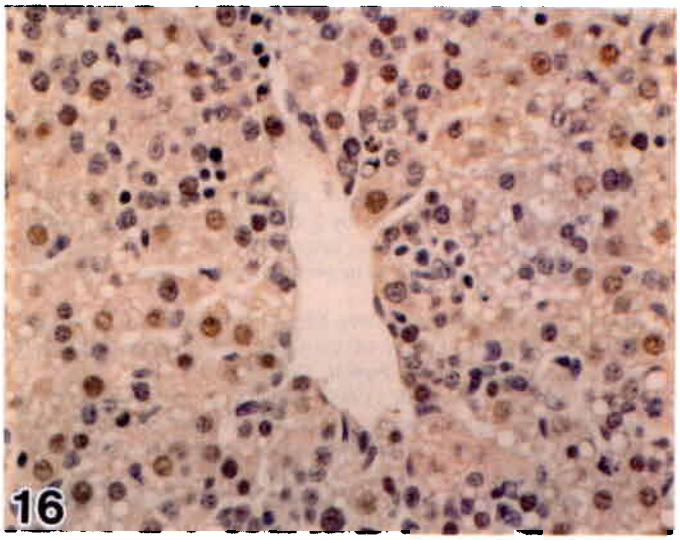

FIG. 16.—Myc expression in most hepatocytes in a 1-wk-old AL-*myc* mouse liver. Immunohistochemical staining for myc protein. ×370.

Expression of the second transgene, AL-*myc*, caused an increase in the extent and persistence of the lesions possibly by a mechanism other than increasing the level of TAg expression. Continuous overexpression of *myc*, even at a level not detected by immunohistochemistry, also accelerated tumor development in AL-TAg mouse liver (8). In the present study, BrdU LIs in 2-wk-old AL-TAg × AL-*myc* bitransgenic mice euthanatized 2 hr after BrdU dosing were generally higher than those in AL-TAg single transgenic mice. Although the number of mice examined is too small (3–6) to demonstrate differences statistically, the data suggest that coexpression of c-*myc* with TAg increased cell proliferation. The c-*myc* oncogene has been reported to be highly expressed in proliferating cells and downregulated by differentiation stimuli (13, 15). The present model may show that manipulation of c-*myc* expression could induce changes in both proliferation and differentiation of hepatic parenchymal cells *in vivo*.

In single transgenic and bitransgenic mice carrying TAg, high BrdU LIs (i.e., high cell proliferation activities) were observed in centrilobular areas. This activity may be related to the prolonged expression of TAg in these areas; TAg is known to have mitogenic activity (9). However, whether or not these high LIs were due to the presence of ductular cells could not be determined because LIs in ductular and nonductular cells could not be obtained separately; thus, the relationship between ductular structure formation and tumor development remained obscure. We also attempted to detect BrdU-positive cells in the livers 3 or 7 days after BrdU pulse dosing because we intended to use BrdU as a possible marker of ductular cells to trace their fate. However, both ductular and nonductular cells were actively proliferating in young (2-wk-old) mice, so that BrdU could not be used to differentially mark specific cell populations.

Despite the fact that duct formation occurs in some hepatic diseases, little information is available on the molecular events associated with this phenotypic alteration or the relationship, if any, to neoplasia. We could not define a causative link between altered differentiation (ductular structure formation) and tumor development in this hepatocarcinogenesis model. Ductular formation may not have played a direct role in hepatic tumor development but rather may have reflected a perturbation in cellular differentiation that was indirectly linked to development of neoplasia. The present study does show, however, that a single genetic manipulation (the presence of a transgene) affects multiple genes governing morphological and functional characteristics of hepatocytes and biliary cells in a coordinated manner, which may indicate the existence of 1 or more key signal transduction pathways whose altered expression is responsible for the change in hepatic parenchymal cell differentiation. Elucidating the underlying molecular changes associated with altered differentiation states should contribute to our understanding of the mechanisms of differentiation of hepatic parenchymal cells.

ACKNOWLEDGMENTS

We thank Drs. Stephen Tsoi, Hideyuki Mannen, and Hideo Gotoh for great help with preparing the albumin probe for *in situ* hybridization and Mr. David Lennard for immunohistochemical staining for myc protein. We also thank Drs. Ann Rodovsky and Robert Sills for critical review of this manuscript.

REFERENCES

1. Araki K, Hino O, Miyazaki J, and Yamamura K (1991). Development of two types of hepatocellular carcinoma in transgenic mice carrying the SV40 large T-antigen gene. *Carcinogenesis* 12: 2059–2062.
2. Brenner DA, Buck M, Feitelberg SP, and Chojkier M (1990). Tumor necrosis factor-alpha inhibits albumin gene expression in a murine model of cachexia. *J. Clin. Invest.* 85: 248–255.
3. Cartier N, Miquerol L, Tulliez M, Lepetit N, Levrat F, Grimber G,

Briand P, and Kahn A (1993). Diet-dependent carcinogenesis of pancreatic islets and liver in transgenic mice expressing oncogenes under the control of the L-type pyruvate kinase gene promoter. *Oncogene* 7: 1413–1422.

4. Cascio S and Zaret KS (1991). Hepatocyte differentiation initiates during endodermal-mesenchymal interactions prior to liver formation. *Development* 113: 217–225.
5. Dunsford HA, Maset R, Salman J, and Sell S (1985). Connection of ductlike structures induced by a chemical hepatocarcinogen to portal bile ducts in the rat liver detected by injection of bile ducts with a pigmented barium gelatin medium. *Am. J. Pathol.* 118: 218–224.
6. Dyer KR and Messing A (1989). Metal-inducible pathology in the liver, pancreas, and kidney of transgenic mice expressing SV40 early region genes. *Am. J. Pathol.* 135: 401–410.
7. Elmore LW and Sirica AE (1991). Phenotypic characterization of metaplastic intestinal glands and ductular hepatocytes in cholangiofibrotic lesions rapidly induced in the caudate liver lobe of rats treated with furan. *Cancer Res.* 51: 5752–5759.
8. Enomoto A, Sandgren EP, and Maronpot RR (1998). Interactive effects of c-*myc* and transforming growth factor α transgenes on liver tumor development in simian virus 40 T antigen transgenic mice. *Vet. Pathol.* 35: 283–291.
9. Fanning E and Knippers R (1992). Structure and function of simian virus 40 large tumor antigen. *Annu. Rev. Biochem.* 61: 55–85.
10. Hanahan D (1988). Dissecting multistep tumorigenesis in transgenic mice. *Annu. Rev. Genet.* 22: 479–519.
11. Hino O, Kitagawa T, Nomura K, Ohtake K, Cui L, Furuta Y, and Aizawa S (1991). Hepatocarcinogenesis in transgenic mice carrying albumin-promoted SV40 T antigen gene. *Jpn. J. Cancer Res.* 82: 1226–1233.
12. Kioussis D, Eiferman F, van de Rijn P, Gorin MB, Ingram RS, and Tilghman SM (1981). The evolution of α-fetoprotein and albumin. II. The structures of the α-fetoprotein and albumin genes in the mouse. *J. Biol. Chem.* 25: 1960–1967.
13. Koskinen PJ and Alitalo K (1993). Role of *myc* amplification and overexpression in cell growth, differentiation and death. *Semin. Cancer Biol.* 4: 3–12.
14. Lemire JM, Shiojiri N, and Fausto N (1991). Oval cell proliferation and the origin of small hepatocytes in liver injury induced by D-galactosamine. *Am. J. Pathol.* 139: 535–552.
15. Marcu KB, Bossone SA, and Patel AJ (1992). *myc* Function and regulation. *Annu. Rev. Biochem.* 61: 809–860.
16. Melhem MF, Meisler AI, Finley GG, Bryce WH, Jones MO, Tribby II, Pipas JM, and Koski RA (1992). Distribution of cells expressing myc proteins in human colorectal epithelium, polyps, and malignant tumors. *Cancer Res.* 52: 5853–5864.
17. Nagore N, Howe S, Boxer L, and Scheuer PJ (1989). Liver cell rosettes: Structural differences in cholestasis and hepatitis. *Liver* 9: 43–51.
18. Palmiter RD and Brinster RL (1986). Germ-line transformation of mice. *Annu. Rev. Genet.* 20: 465–499.
19. Rosario MO, Perkins SL, O'brien DA, Allen RL, and Eddy EM (1992). Identification of the gene for the developmentally expressed 70 kDa heat-shock protein (P70) of mouse spermatogenic cells. *Dev. Biol.* 150: 1–11.
20. Rüther U, Woodroofe C, Fattori E, and Ciliberto G (1992). Inducible formation of liver tumors in transgenic mice. *Oncogene* 8: 87–93.
21. Saber MA, Novikoff PM, and Shafritz DA (1990). Albumin and collagen mRNA expression in normal and analbuminemic rodent liver: Analysis by *in situ* hybridization using biotinylated probes. *J. Histochem. Cytochem.* 38: 199–207.
22. Sandgren EP, Quaife CJ, Pinkert CA, Palmiter RD, and Brinster RL (1989). Oncogene-induced liver neoplasia in transgenic mice. *Oncogene* 4: 715–724.
23. Schirmacher P, Held WA, Yang D, Biempica L, and Rogler CE (1991). Selective amplification of periportal transitional cells precedes formation of hepatocellular carcinoma in SV40 large Tag transgenic mice. *Am. J. Pathol.* 139: 231–241.
24. Sepulveda AR, Finegold MJ, Smith B, Slagle BL, DeMayo JL, Shen RF, Woo SLC, and Butel JS (1989). Development of a transgenic mouse system for the analysis of stages in liver carcinogenesis using tissue-specific expression of SV40 large T-antigen controlled by regulatory elements of the human α-1-antitrypsin gene. *Cancer Res.* 49: 6108–6117.
25. Sirica AE, Cole SL, and Williams T (1994). A unique rat model of bile ductular hyperplasia in which liver is almost totally replaced with well-differentiated bile ductules. *Am. J. Pathol.* 144: 1257–1268.
26. Sirica AE and Williams TW (1992). Appearance of ductular hepatocytes in rat liver after bile duct ligation and subsequent zone 3 necrosis by carbon tetrachloride. *Am. J. Pathol.* 140: 129–136.
27. Thung SN (1990). The development of proliferating ductular structures in liver disease. An immunohistochemical study. *Arch. Pathol. Lab. Med.* 114: 407–411.
28. Ton TT, Foley JF, Flagler ND, Gaul BW, and Maronpot RR (1997). Feasibility of administering 5-bromo-2′-deoxyuridine (BrdU) in drinking water for labeling S-phase hepatocytes in mice and rats. *Toxicol. Methods* 7: 123–136.
29. Tulchin N, Ornstein L, Guillem J, O'Toole K, Lambert ME, and Weinstein IB (1988). Distribution of the c-myc oncoprotein in normal and neoplastic tissues of the rat colon. *Oncogene* 3: 697–701.
30. Vandersteenhoven AM, Burchette J, and Michalopoulos G (1990). Characterization of ductular hepatocytes in end-stage cirrhosis. *Arch. Pathol. Lab. Med.* 114: 403–406.
31. Van Eyken P, Sciot R, and Desmet VJ (1988). A cytokeratin immunohistochemical study of alcoholic liver disease: Evidence that hepatocytes can express 'bile duct-type' cytokeratins. *Histopathology* 13: 605–617.
32. Van Eyken P, Sciot R, and Desmet VJ (1989). A cytokeratin immunohistochemical study of cholestatic liver disease: Evidence that hepatocytes can express 'bile duct-type' cytokeratins. *Histopathology* 15: 125–135.
33. Watanabe M, Muramatsu T, Shirane H, and Ugai K (1981). Discrete distribution of binding sites for *Dolichos biflorus* agglutinin (DBA) and for peanut agglutinin (PNA) in mouse organ tissues. *J. Histochem. Cytochem.* 39: 779–790.